Hindawi Publishing Corporation
Advances in Materials Science and Engineering
Volume 2016, Article ID 9856474, 12 pages
http://dx.doi.org/10.1155/2016/9856474

*Research Article*

# Off-Axial Tensile Properties of Precontraint PVDF Coated Polyester Fabrics under Different Tensile Rates

**Lanlan Zhang**

*College of Construction Management, Jiangsu Vocational Institute of Architectural Technology, Xuzhou 221116, China*

Correspondence should be addressed to Lanlan Zhang; zhanglanlan007@163.com

Received 30 March 2016; Revised 2 June 2016; Accepted 19 June 2016

Academic Editor: Gonzalo Martínez-Barrera



Two types of Precontraint PVDF coated polyester are taken as the research objects. A series of uniaxial tensile tests were carried out to study the tensile performances of the specimens in eleven in-plane directions including 0°, 5°, 15°, 25°, 35°, 45°, 55°, 65°, 75°, 85°, and 90°, and six tensile rates (10 mm/min, 25 mm/min, 50 mm/min, 100 mm/min, 200 mm/min, and 500 mm/min) were also considered. The corresponding failure modes and fracture mechanisms were discussed, and the relationships between tensile strength and strain at break and tensile rate and off-axial angles were obtained. Results show that the Precontraint PVDF coated woven fabrics are typically anisotropic. With off-axial angle increasing, the tensile strength decreases while the strain at break increases. Three failure modes can be observed, including failure of yarns pulled out, yarns fracture, and mixture failure. With tensile rate increasing, the tensile strength increases slightly while the strain at break decreases. The tensile strength and strain at break show good linear relationship with tensile rate's logarithm.

## 1. Introduction

Membrane structure is a new structural system developed in the middle of 20th century. It is welcomed by the architects, engineers, and others, due to complex architectural forms and special mechanical properties [1–3]. Its structural stiffness can be obtained by tensioning the membrane surface, together with the curvature forms. The design membrane prestress is strongly related to the curvature forms of membrane surface. Whether the accuracy of membrane prestress can satisfy the design requirements may directly affect the construction accuracy, even the structure safety [4].

Coated fabric is a principal material used in membrane structures. It can only resist tensions, almost without any flexural resistance. As shown in many existing literatures, for plain woven polyester coated with PVDF, the differences between the mechanical properties of the warp and the weft are significant. The unbalanced woven structure of the materials results in the unbalanced deformations of membrane materials. When the warp stress is less than the weft stress, negative strain in the warp direction may reduce the application efficiency of the material. However, it is often beneficial for installation for a fabric to be unbalanced so that it can be tensioned in the weft direction and prestress is induced in the warp direction by interaction of the yarns. Then, the Precontraint woven technology was proposed by the Serge Ferrari Company. A more stable fabric can be obtained by applying tension to warp and weft of a plain woven fabric, in order to obtain more consistent and more balanced warp and weft stiffness through the cloth. Until now, there are only a few of references about the mechanical properties of PVDF coated polyester with the Precontraint technology. Ambroziak carried out series of tests on the mechanical behaviors under different loading protocols, such as monotonous loading, cyclic loading, and others [5–8]. The main mechanical parameters including tensile strength, elastic modulus, and Poisson ratio are obtained. However, there are few literatures about the failure mechanisms and strength criterion of Precontraint coated fabrics. Zhang et al. conducted the off-axial tensile tests on the Precontraint PVDF coated polyester with the tensile rate of 100 mm/min and analyzed the corresponding failure mechanisms [9].

As we know, the failure mechanisms and strength criteria are important for the design and analysis of membrane structures. Considering the stress states in practical engineering, the biaxial tests may be the best method to solve

this question. However, it is difficult to find the suitable specimens for the tests. There are some previous references about the failure tests of the coated fabrics [10–13]. However, until now, the failure strength obtained in those references is only the failure strength of biaxial specimens, not the failure strength of this material. Nowadays, the off-axial test may be the most suitable method to analyze the failure mechanism of coated fabrics, although it can only produce some simple stress states. Some researchers have used the off-axial tests to analyze the failure mechanisms and strength criteria of coated fabrics. The off-axial tests always contain seven bias angles, including 0°, 15°, 30°, 45°, 60°, 75°, and 90° [13–15]. The results indicate that the material strength decreases significantly under the interaction of shear and tensile, especially for the bias angles from 0° to 15° or 90° to 75°. This phenomenon cannot be accurately described by the current strength criteria, in which the shear stress plays an important role in this aspect [16–18]. Therefore, it is necessary to reduce the angle gap of off-axial tests to study the failure mechanism of coated fabrics further.

Just as shown in previous references, the current researches are mainly on the mechanical properties of coated fabrics under the standard test conditions recommended in the codes or the specifications. However, as anisotropic polymer composites, the loading protocols may have significant effects on the mechanical properties of coated fabrics [4–6, 8, 19–21].

The wind-borne debris always hits the surface of membrane structures and the microcrack may appear in the membrane surface. Under harsh environments, the microcrack can easily propagate and lead to the overall failure of membrane structures due to low tear strength. The membrane structures are always the landmark and their failure will bring economic loss and huge social impacts. The rate-dependent mechanical properties of coated fabrics are an important basis of design and analysis of membrane structures. There are a lot of references about the viscoelastic properties of coated fabrics under low strain rates [22–28]. Some classical viscoelastic models are proposed for the construction analysis and the determination of shrinkage ratio in the pattern cutting analysis [29–31]. Meanwhile, there are fewer references about the material response under dynamic loading. However, the structural response under dynamic loading with high rates is also very important for the design, for example, the analysis of wind-induced disasters. Therefore, it is necessary to study the mechanical properties and failure mechanisms of coated fabrics under different tensile rates.

This paper presented the off-axial tensile behaviors and failure mechanisms of Precontraint PVDF coated polyester, in which the effects of tensile rate on the mechanical parameters and failure modes are discussed.

## 2. Materials and Methods

The Precontraint PVDF coated polyester Ferrari 1002 T2 and 702 T2 are taken as the research objects, as shown in Table 1. They are plain woven by the Precontraint technology with PVDF top coats in both sides. The Precontraint technology holds the textile under tension in both warp and weft directions throughout the manufacturing process to ensure higher levels of dimensional stability and tensile strength, less elongation, and a flatter base cloth. This enables a more substantial protective coating to be placed on top of the yarn without increasing overall thickness, creating a flatter, lighter textile subject to less deformation under tension. It is with good durability and self-cleaning, which can be used in permanent structures.

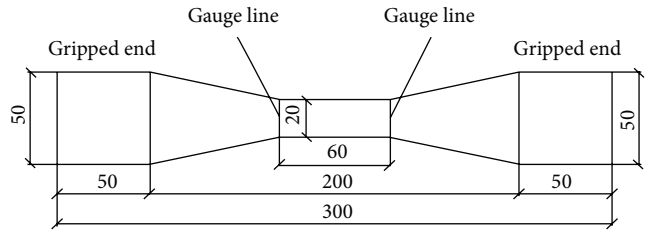


Figure 1: Dimensions of dumbbell specimens.

The uniaxial tests are carried out using the electromechanical universal testing machine with temperature box. The strip specimens are always used in the off-axial tests. However, the failure always appears in the gripped ends, for example, fracture or slippage, and then the test data is invalid. Therefore, the dumbbell specimens are used in this test, as shown in Figure 1. The stress is got by dividing the tensile forces by the area of cross-section in the middle. The strain is got by the displacement measurement.

## 3. Results and Discussions

*3.1. Comparisons of Strip Specimens and Dumbbell Specimens.* Here, this part also presents the comparisons of dumbbell and strip specimens under the off-axial tensile tests by the finite element analysis. In the finite element analysis, the orthotropic constitutive relation is used and the elastic modulus in warp and weft is 600 MPa and 400 MPa, respectively. The strip specimens are prepared according to German codes DIN 53334 [32]. The width is 50 mm, the length is 300 mm, and the original gage length is 200 mm. The pattern equality of samples is important for the test results.

The comparisons of the stress distributions of dumbbell and strip specimens are shown in Figure 2. For strip specimens, it can be observed that the stress in the gripped ends is high and the slippage always appears before the fracture of materials. This is also related to the smooth surface of PVDF coating. This phenomenon is consistent with the tensile tests. For dumbbell specimens, in the effective area, the stress distribution is consistent with that of strip specimens. The width of gripped ends is larger than that of the effective area. It can afford enough fractional force to avoid the slippage of specimens. The maximum stress always appears in the effective area and the test data is valid. If the failure does not appear in the effective area, the test data can be considered as invalid.

*3.2. Uniaxial Tensile Curves.* Due to the same woven method, the variation trends of tensile behaviors of two materials (702

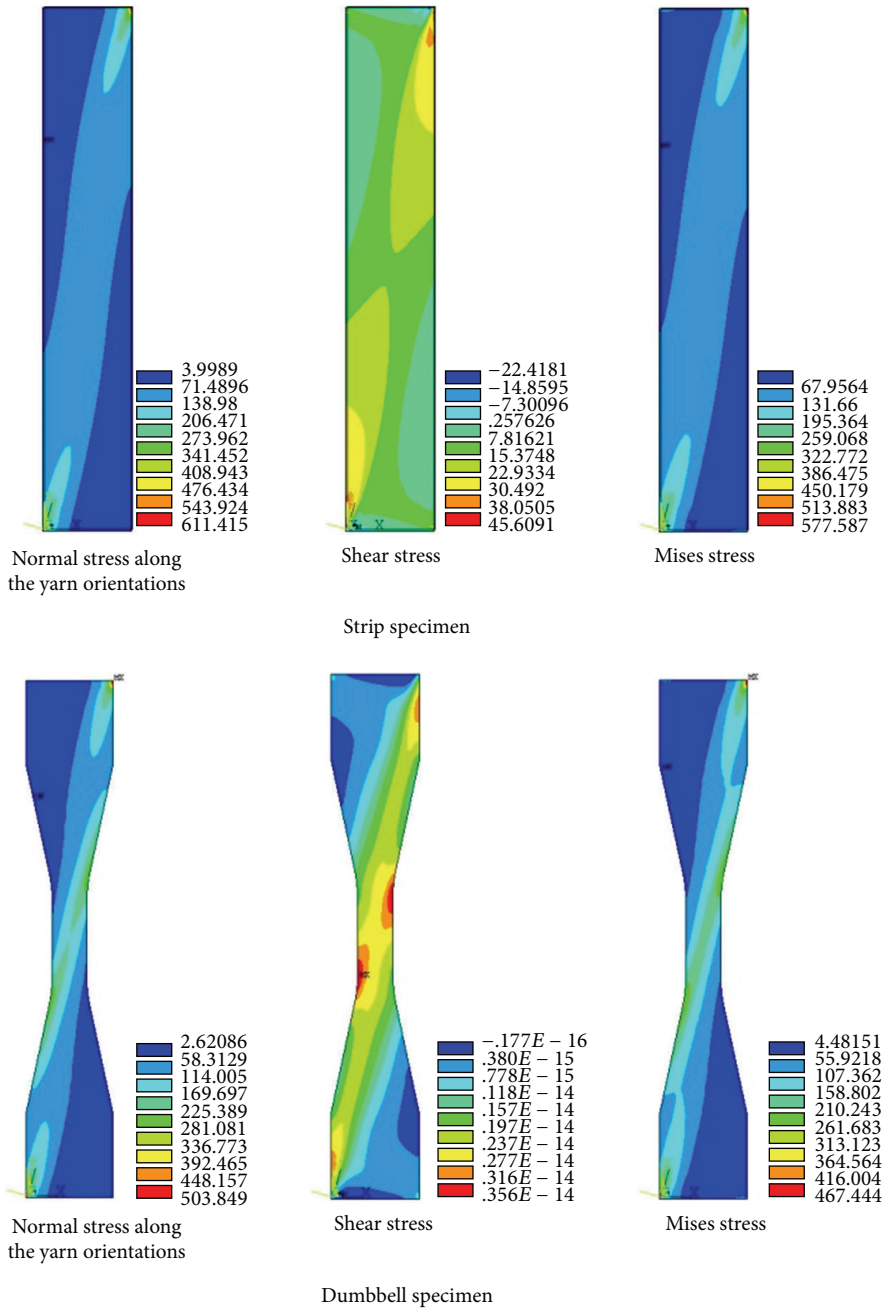


Figure 2: Stress distribution of 15-degree specimens.

T2 and 1002 T2) are similar. Therefore, limited by the layout, this part only presents the test results of Precontraint 702 T2, as shown in Table 2.

First, the tensile behaviors under the tensile rate of 100 mm/min are taken as the research object, because 100 mm/min is the recommended tensile rate in current codes/specifications [1]. The angles 0° and 90° are the weft and the warp, respectively. Figure 3 shows that the Precontraint PVDF coated polyester performs typically orthotropic. The differences between the tensile strength in the warp and in the weft are not so significant as those of the plain wove fabrics, which is related to the woven densities and woven methods [33]. Then, for Precontraint coated fabrics, the pretension is applied to the warp and weft of yarns and a more consistent and more balanced warp and weft stiffness through the cloth are obtained. For the on-axial specimens, part of yarns fracture first and the unloading will be transferred to the adjacent yarns. Due to high adhesive strength, the yarns are difficult to be pulled out from the coating/substrate interface, and most of yarns fracture at the same section. Then, the main failure modes are even failure, which is "yarn fracture" (Figure 4). When the bias angle is 85° and 5°, there will be a significant decrease compared with those of on-axial specimens. Although the number of yarns in the effective

Table 1: Specifications of test materials.

| Type | Manufacturer | Weight g/m$^2$ | Thickness mm | Yarn density dtex PES HT | | Tensile strength kN/m | | Tear strength N | |
|---|---|---|---|---|---|---|---|---|---|
| | | | | Warp | Weft | Warp | Weft | Warp | Weft |
| Ferrari 1002 T2 | Serge Ferrari | 1050 | 0.78 | 1100 | 1100 | 84.0 | 80.0 | 500 | 460 |
| Ferrari 702 T2 | | 750 | 0.56 | 1100 | 1670 | 60.0 | 56.0 | 300 | 280 |

Table 2: Off-axial test results of Precontraint 702 T2 (100 mm/min).

| Angle | Tensile strength/(kN·m$^{-1}$) | | Strain at break/% | |
|---|---|---|---|---|
| | Average value | Standard deviation | Average value | Standard deviation |
| 0° | 58.051 | 3.444 | 13.541 | 0.154 |
| 5° | 50.542 | 1.633 | 12.662 | 0.061 |
| 15° | 44.834 | 0.864 | 18.072 | 0.760 |
| 25° | 39.271 | 1.664 | 32.556 | 0.363 |
| 35° | 38.081 | 1.827 | 38.992 | 0.338 |
| 45° | 37.709 | 0.733 | 40.416 | 0.189 |
| 55° | 37.981 | 0.198 | 39.101 | 0.348 |
| 65° | 40.771 | 0.908 | 32.662 | 0.144 |
| 75° | 45.934 | 0.945 | 21.441 | 0.201 |
| 85° | 51.339 | 2.345 | 14.100 | 0.126 |
| 90° | 58.699 | 0.966 | 14.446 | 0.125 |

area remains almost unchanged, the application ratio of yarns decreases significantly under the tensile-shear interaction. In the fracture section, most of the yarns facture even and part of yarns are pulled from the adjacent yarn-coating interface. Additionally, the strain at break may be lower than that of the on-axial specimens.

When the bias angle increases, for example, the specimens with bias angles of 75°, 15°, 65°, and 25°, the tensile strength decreases and the strain at break increases. The failure modes are the mid-section fracture and part of adjacent yarns are pulled out. Compared with the specimens with smaller bias angles (85° and 5°), the number of pulled-out yarns increases and the number of fractured yarns decreases. Therefore, the strain at break increases significantly and the fracture section is uneven. When the bias angles are 55, 35, and 45, the tensile strength is the lowest and the strain at break is the highest. Then, the failure mode is "interface failure," as shown in Figure 4(b). The coating can constrain the deformation of yarns, which is in favor for the loading capacity of coated fabrics. The shear force plays a dominant role in the material failure. The "yarns pulled out" is the main failure mode.

In the off-axial tests, there are two types of yarns, complete ones and incomplete ones. With bias angle increasing, the number of incomplete yarns remains unchanged, while the number of complete ones decreases. From Figure 5, due to high shear force, the incomplete yarns are easily pulled out and then the tensile strength decreases significantly. When the bias angle increases from 15° to 25° (or 75° to 65°), the number of complete yarns decreases to 0. Then, the tensile stress decreases and the shear stress increases, but the decreasing of tensile strength is not very obvious. When the bias angle increases from 25° to 45° (or 65° to 45°), the shear stress gradually becomes the dominant and the shear failure is observed.

According to the SEM image shown in Figure 6(a), the fracture cross-section is even fracture in the failure mode "yarns even fracture." The fiber bundles parallel to the loading direction show even fracture. Figure 6(b) is typically mixed failure. The middle part of the fiber bundles perform uneven fracture, while the sides are pulled out, accompanied by the damage of a small amount of coating. For the failure mode "yarns pulled out" (Figure 6(c)), the fiber bundles are completely pulled out, and then the coating is serious damage.

*3.3. Loading Rate.* Figure 7 shows that the effect of tensile rate on the material tensile strength is obvious and the tensile strength increases with tensile rate increasing. The least square method is used to fit the mechanical parameters (tensile strength and strain at break) under different tensile rates. The black points are experiment data, and the line is the fitting results. As shown in Figure 8, with tensile rate increasing, the tensile strength increases about 5%–15%, and the strain at break decreases about 5%–10%. Figure 8 shows the material tensile strength and strain at break shows a good linear correlation with the tensile rate's logarithm.

As shown in Figure 8, the relationship between tensile strength, strain at break, and tensile rate is as follows:

$$f_u = a + b \lg v_\varepsilon,$$
$$\varepsilon_u = c + d \lg v_\varepsilon, \quad (1)$$

where $f_u$ is material tensile strength, kN·m$^{-1}$, $\varepsilon_u$ is strain at break, %; $v_\varepsilon$ is tensile rate, mm/min; $a$, $b$, $c$, and $d$ are the parameters that have no physical meanings. The parameters

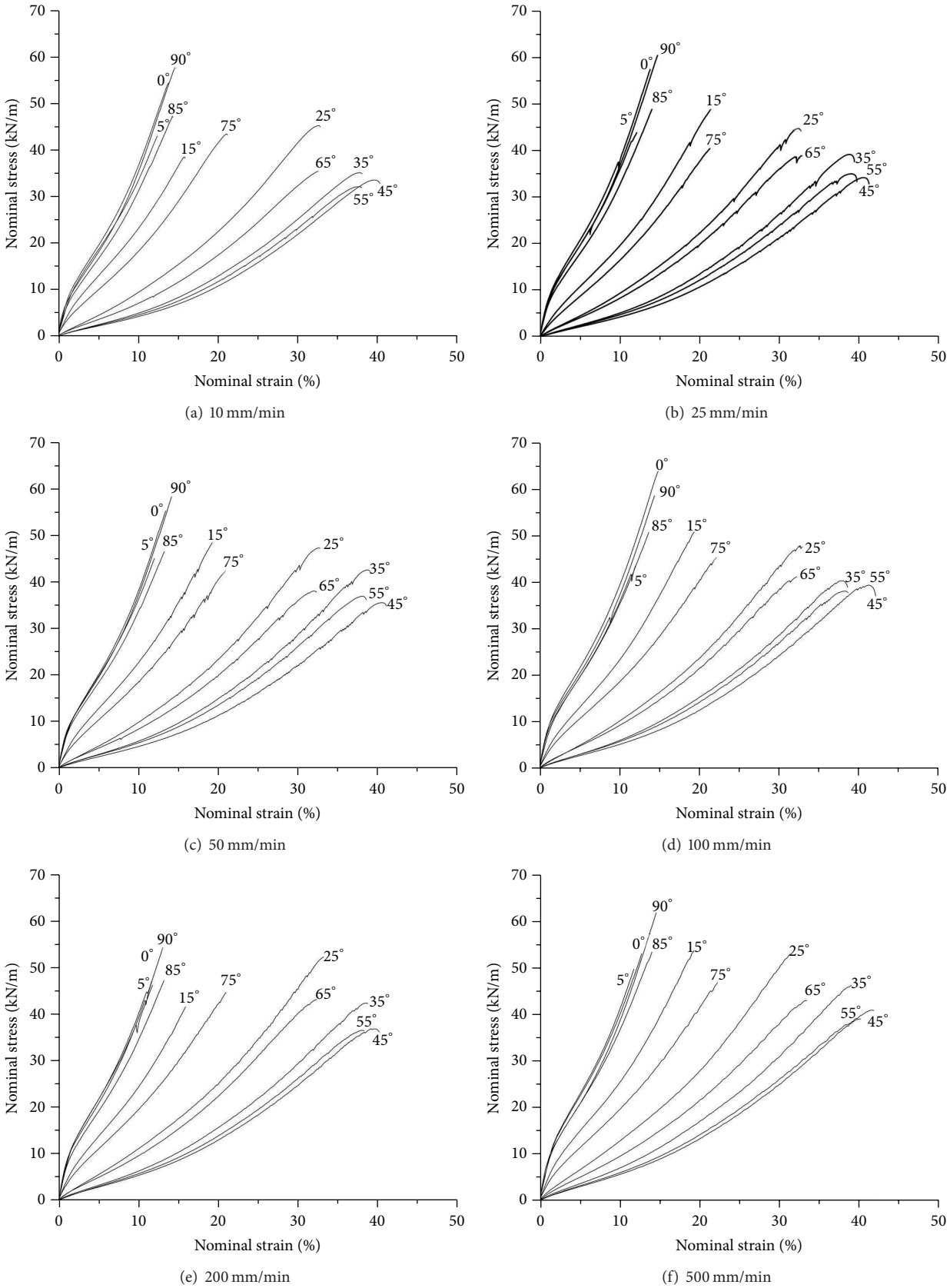


(a) 10 mm/min

(b) 25 mm/min

(c) 50 mm/min

(d) 100 mm/min

(e) 200 mm/min

(f) 500 mm/min

Figure 3: Off-axial tensile curves of Precontraint 702 T2 under different loading rates.

(a) Even fracture failure (0°) (b) Yarns pulled out (45°) (c) Mixed failure (5°)

Figure 4: Failure modes of Precontraint 702 T2.

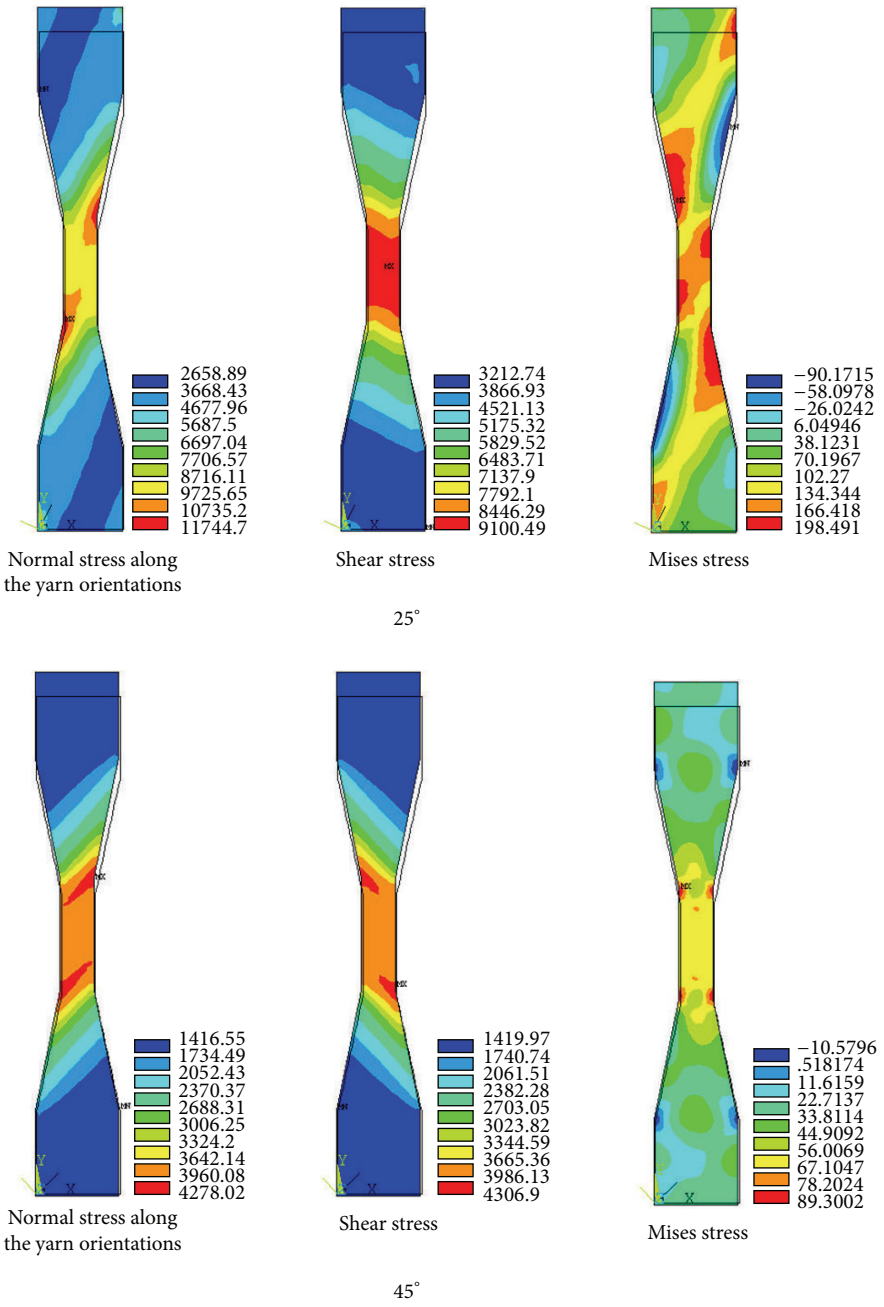


Figure 5: Finite element analysis of off-axial tensile test (Precontraint 702 T2).

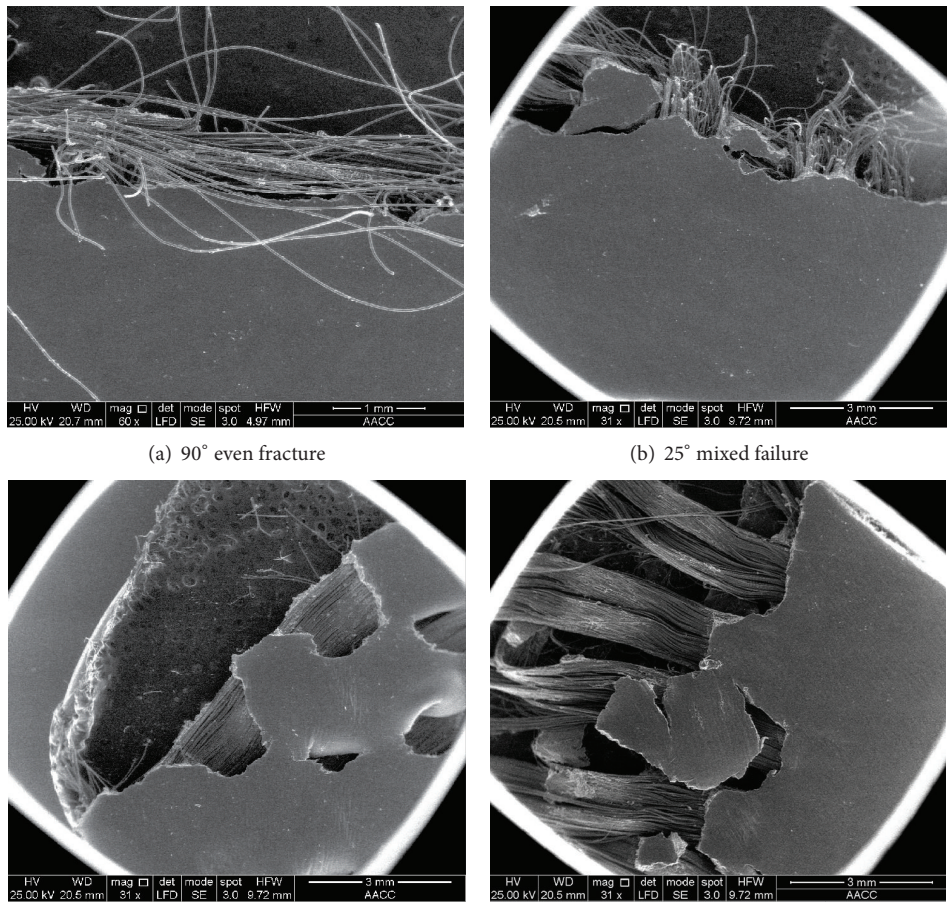

(a) 90° even fracture

(b) 25° mixed failure

(c) 45° interface failure

Figure 6: SEM images of fractographics of off-axial specimens.

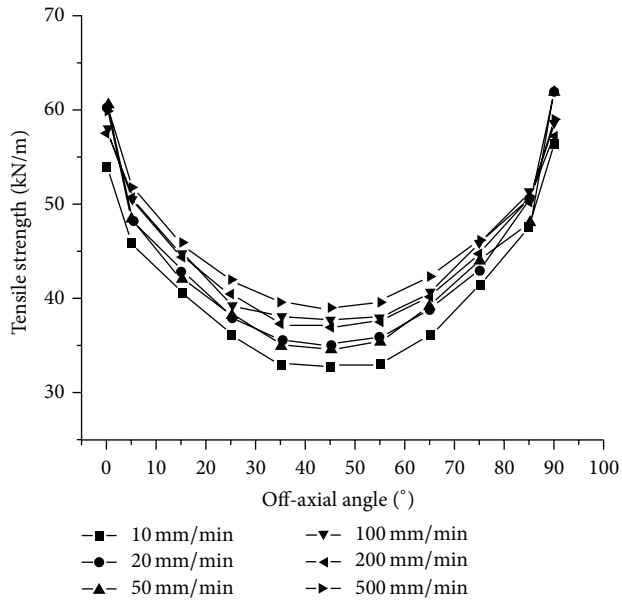


Figure 7: Off-axial tensile strength of Precontraint 702 T2 under different loading rates.

can be obtained by fitting the experimental data, as shown in Table 3. The tensile strength and strain at break under different tensile rates can be predicted by using the above equations, which can be used for the mechanical behaviors of membrane structures under different tensile rates. Besides, the wind-induced disasters are the main reason for the failure of membrane structures. The tensile strength increases with tensile rate increasing, which is favorable for the safety of membrane structures under high rate winds, for example, typhoon. Using the tensile strength obtained by the standard inspection method with the tensile rate of 100 mm/min is conservative and can increase the safety reliability of membrane structures.

As shown in Figure 8, for the specimens with the same bias angles, the failure modes regarding different loading rates are almost the same. With bias angle increasing, the failure modes change from "even fracture" to "mixed failure." Finally, the main failure mode is yarns pulled out, when the bias angle is 45 degrees. With tensile rate increasing, the deformation energy of membrane materials increases and the rate of energy absorption increases. Therefore, the material fracture toughness increases and the ultimate total

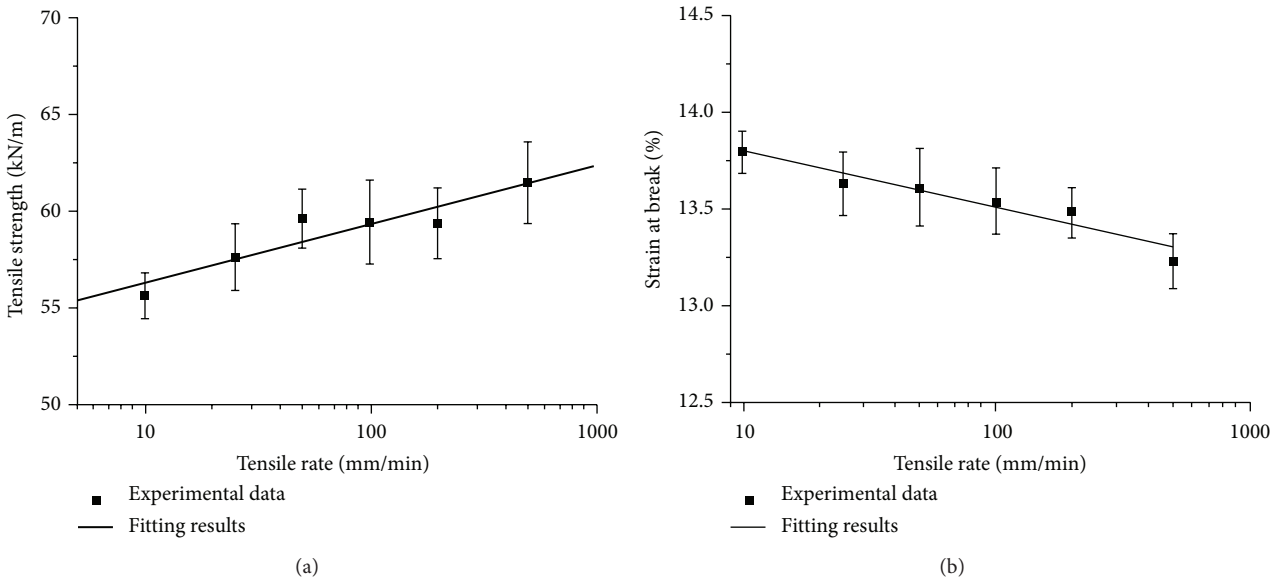


Figure 8: Relationship between tensile strength and strain at break and tensile rate.

Table 3: Relationship between tensile strength & strain at break and tensile rate.

| Bias angle/° | $a$ | $b$ | $c$ | $d$ |
|---|---|---|---|---|
| 0 | 55.113 | 1.779 | 14.092 | −0.293 |
| 5 | 46.188 | 1.941 | 12.812 | −0.068 |
| 15 | 38.001 | 2.976 | 19.490 | −0.654 |
| 25 | 32.978 | 3.256 | 33.107 | −0.401 |
| 35 | 29.863 | 3.288 | 39.739 | −0.335 |
| 45 | 29.553 | 3.488 | 41.608 | −0.621 |
| 55 | 30.042 | 3.546 | 39.302 | −0.181 |
| 65 | 32.402 | 4.147 | 33.462 | −0.386 |
| 75 | 39.338 | 2.654 | 22.206 | −0.409 |
| 85 | 48.87 | 0.674 | 14.792 | −0.397 |
| 90 | 58.496 | 0.189 | 14.903 | −0.253 |

energy of membrane fracture increases, which will lead to the increasing of membrane tensile strength. Meanwhile, with tensile rate increasing, the material resistance to crack propagation increases, while the strain at break decreases slightly [14]. It can be observed that when the tensile rate is low, the effect of microflaws on material tensile strength is significant. Here, the "mixed failure" is taken as the example. When the tensile rate is low, the side yarns are easily pulled out from the adjacent yarns or the coating/yarn interface. The failure always appears in the boundary, part of yarns are pulled out, and the mid-section of membrane materials fractures finally. With tensile rate increasing, fewer yarns are pulled out and more yarns fracture. Then, most of the mid-section fractures and fewer of yarns are pulled out. During the failure process, the coating plays an important role in the failure mechanisms. The coated fabric is composed of the coating and the substrate, while the stress wave may pass with different rates in the coating and the substrate. The substrate carries most of the force and the coating carries less. Then, the coating may restrain the deformation of substrates, due to smaller deformation. Therefore, when the tensile rate is low, the material fracture toughness and the resistance to crack propagation are low. Then, the microcrack can easily propagate and lead to the failure of materials. When the tensile rate is high, the resistance to crack propagation provided by the coating increases, while there is not enough time to achieve the ultimate deformation. Then, the crack propagates slowly and the tensile strength increases, because the limit strain energy remains almost unchanged. This is also why the strain at break decreases.

It should be noted that there are slight differences on the failure modes under different loading rates. As shown in Figure 9, when the tensile rate is low, it can be seen that some of yarns fracture while the other yarns are pulled out. When the tensile rate is high, more yarns fracture while fewer yarns are pulled out. This is mainly related to the interface strength, which is associated with the frictions between the longitudinal yarns and the transverse yarns and the frictions between the substrate and the coating [34, 35]. Besides, it may be related to the microdefects in the coated fabrics due to the manufacture and construction process. The failure modes are related to the distributions of microdefects. When the tensile rate is low, the microscopic defects can easily develop to macroscopic slits/cracks under tensile loading. It may lead to the interactions of many slits, which is a complex failure mode. This cannot be predicted by the macroscopic strength criteria. It can only be described by the damage mechanics based on the microscopic structures of coated fabrics.

## 4. Strength Criterion

As the expansion of the failure criterion for homogeneous materials, the macroscopic strength criteria of composites are

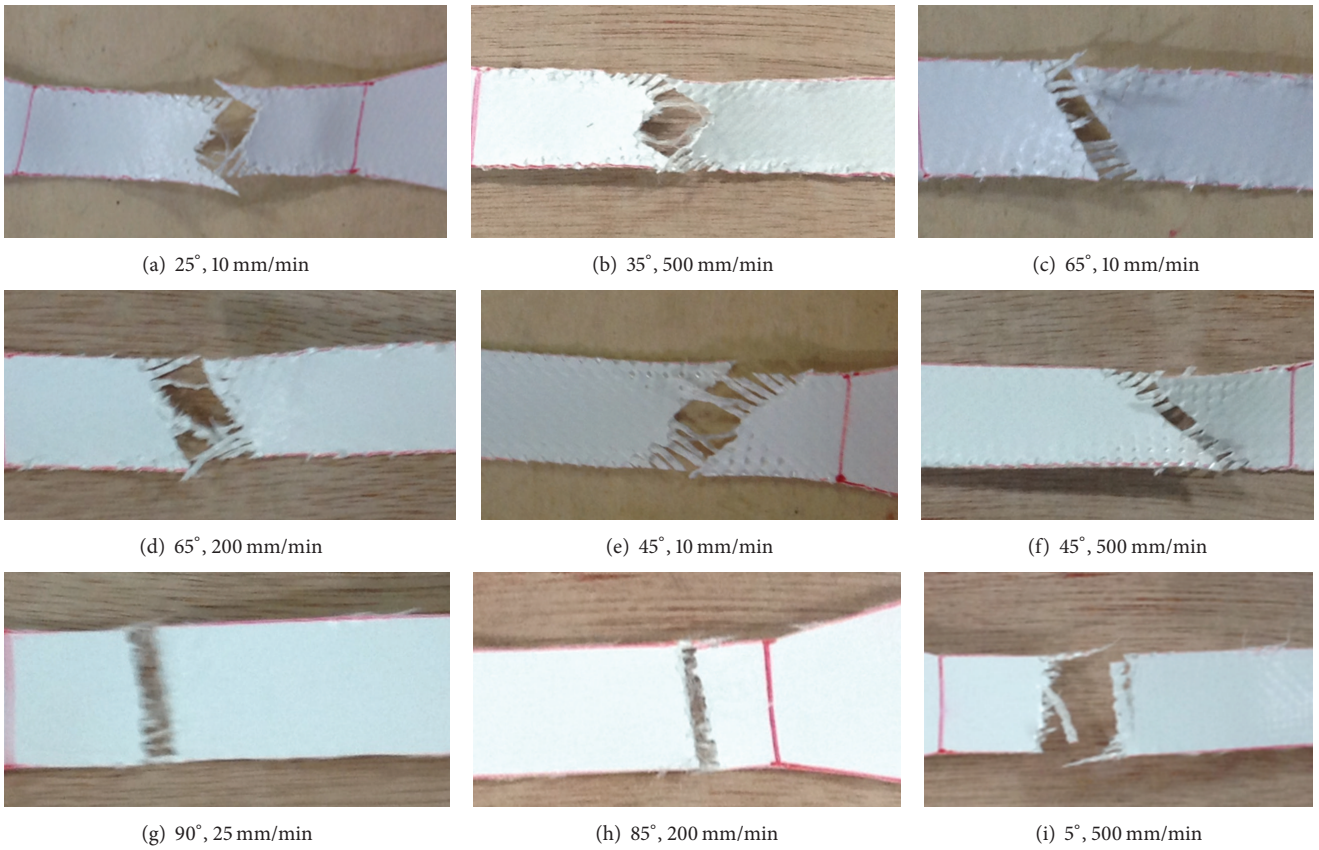

(a) 25°, 10 mm/min (b) 35°, 500 mm/min (c) 65°, 10 mm/min

(d) 65°, 200 mm/min (e) 45°, 10 mm/min (f) 45°, 500 mm/min

(g) 90°, 25 mm/min (h) 85°, 200 mm/min (i) 5°, 500 mm/min

Figure 9: Failure modes of PVDF coated woven fabrics under different tensile rates.

popular due to operationally simple expressions. For engineering design, prediction accuracy and simple expressions are two important aspects of failure criteria. Among the current strength criteria, the quadratic criteria are recommended by many researchers, because they are single valued functions with smooth and continuous failure envelope, particularly suitable for the numerical solution [36–40].

For building coated fabric, it is similar to a plane anisotropic material, of which the mechanical properties in the $Z$ direction (thickness) are always ignored. When predicting the failure strength of building coated fabrics, the failure criteria for three-dimensional composites materials should be degenerated into a two-dimensional criterion.

Here, several classical strength criteria are chosen to predict the tensile strength of off-axial samples, including Tsai-Hill criterion, Yeh-Stratton criterion, Hashin criterion, and Zhang criterion [13, 37, 41, 42]. They are shown as follows:

Tsai-Hill criterion is

$$\frac{\sigma_x^2}{X^2} + \frac{\sigma_y^2}{Y^2} - \frac{\sigma_x \sigma_y}{X^2} + \frac{\tau_{xy}^2}{S^2} = 1. \tag{2}$$

Yeh-Stratton criterion is

$$\frac{\sigma_x}{X} + \frac{\sigma_y}{Y} - \frac{\sigma_x \sigma_y}{X^2} + \frac{\tau_{xy}^2}{S^2} = 1. \tag{3}$$

Hashin criterion is

$$\left(\frac{\sigma_{11}}{X}\right)^2 + \left(\frac{\tau}{S}\right)^2 = 1. \tag{4}$$

Zhang criterion is

$$\frac{\sigma_x}{X} + \frac{\sigma_y}{Y} + \frac{\tau_{xy}}{S} + F_{12}\frac{\sigma_x \sigma_y}{XY} + F_{16}\frac{\sigma_x \tau_{xy}}{XS} = 1, \tag{5}$$

where $\sigma_x$ and $\sigma_y$ are the normal stress in weft and warp, $\tau$ is the shear stress, $X$ and $Y$ are the tensile strength in weft and warp, and $S$ is the shear strength.

Figure 10 shows the comparison between experiment results and the predictions of several existing strength criteria. In most cases, the current strength criteria can make a good prediction of the failure strength of Precontraint PVDF coated fabric. However, slight deviations appear in the tests of small off-axial angles, such as 15° and 75°. This is perhaps because of the crimp interchange in the weaving and coating processes.

In the Tsai-Hill criterion and the Yeh-Stratton criterion, the parameter $F_{12}$ (the interaction item of $\sigma_x$ and $\sigma_y$) is only associated with longitudinal strength $X$. Meanwhile, in the Norris criterion, it is related to the longitudinal strength $X$ and the transverse strength $Y$. For plain woven fabrics, the differences between them are not as significant as that in unidirectional reinforced fabrics. It is an important,

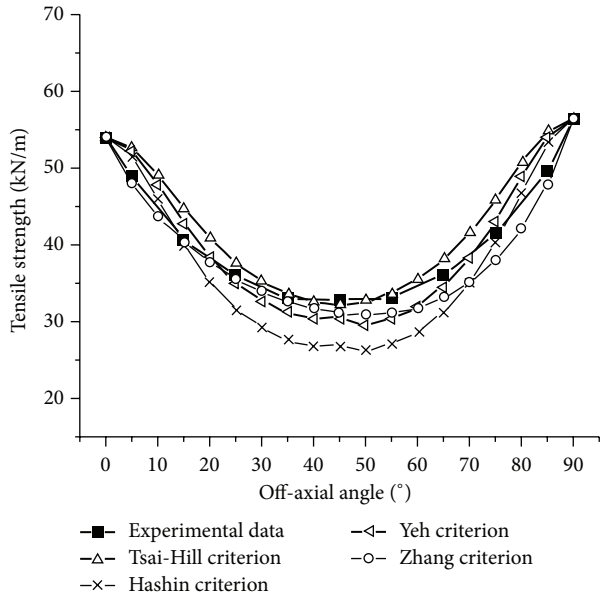


Figure 10: Comparison of experiment data and predictions of several existing strength criteria.

independent but constrained strength component. It is very sensitive in biaxial tests and can be approximately got in such biaxial tests. The determination of the value of $F_{12}$ can be achieved through infinite number of combined-stress states. Comparisons are made with optimum values obtained from least-squares analyses. The value of $F_{12}$ is always small but not ignored. Besides, the parameter $F_{16}$ (the interaction term of normal stress and shear stress) cannot be ignored, especially for the samples with small off-axial angles.

As orthotropic materials, the mechanical properties of the coated fabrics are affected by the bias angles, just as shown in Figure 10. The tensile strength of the on-axial specimens (0 and 90 degrees) is the highest, while that of 45° specimen is the lowest. Therefore, the warp and weft yarns should be located along the principal stress. If not, the ultimate loading capacity of the membrane structure will decrease and the wrinkling may appear under extreme loadings. This should be considered in the form-finding analysis and the cutting pattern design. Under harsh environments, the microcrack in the coated fabrics can easily propagate and lead to the overall failure of membrane structures due to low tear strength. From the above analysis, the tensile strength will increase slightly under high loading rates, which is favorable for the design of membrane structures under high loading rates, for example, the analysis of wind-induced disasters.

Finally, coated fabric is not a continuous homogeneous material in meso- or microscales. In the process of weaving and coating, the yarns and coating are aligned regularly depending on the weaving method. Therefore, in the macroscale, it can be taken into account as a homogeneous material. This is why most of the data can agree well with the predictions of current macroscopic strength criteria. The transfer of force in coated fabrics is mainly through the yarns. The failure always appears at the weakest point and propagates quickly through the yarns. Therefore, the traditional quadratic criteria may not reflect the failure mechanisms of coated fabrics. Further research should be carried out to obtain a simplified equation, which is based on the microscopic structural analysis.

## 5. Conclusions

(1) The Precontraint PVDF coated polyester is typically anisotropic. With bias angle increasing, the tensile strength decreases and the strain at break increases. The warp tensile strength is slightly higher than that in weft, while the strain at break is lower than that in weft. There are not significant differences between the warp and the weft, which is different from the plain woven materials. This is related to the Precontraint woven methods and the woven densities.

(2) The tensile strength is mainly related to failure modes and substrate structure. When the bias angle is 0° and 90°, the tensile stress is the dominant, and the main failure mode is "yarns even fracture." Then, the tensile strength is the highest and the application ratios of yarns are the highest. When the bias angles are close to 45°, the material failure is yarns pulled out, which is the interface failure. The shear stress is dominant and the tensile strength is the lowest. In the intermediate angles, the main failure mode is mixed failure, including yarns fracture and interface failure.

(3) With tensile rate increasing, the tensile strength increases while the strain at break decreases. The tensile strength shows good linear relationship between tensile rate's logarithms. With tensile rate increasing, the deformation energy of coated fabrics increases quickly, while the constraint of coating on material deformation increases. There are slightly differences on the failure modes under different loading rates. Besides, it may be related to the microdefects in the coated fabrics due to the manufacture and construction process.

(4) Most of the current strength criterion can make a better prediction of the material off-axial strength, except for the specimens of 15° and 75°. This is perhaps related to complex failure modes and woven structures. The traditional strength criteria are always based on the homogeneous materials, while the coated fabrics are actually the composition of yarns and substrate.

## Competing Interests

The author declares that there is no conflict of interests regarding the publication of this paper.

## Acknowledgments

This work is supported by Research Program of Jiangsu Vocational Institute of Architectural Technology (Grant no. JYA14-09).

## References

[1] B. Forster and M. Mollaert, *European Design Guide for Tensile Surface Structures*, TensiNet, 2004.

[2] T. D. Dinh, A. Rezaei, W. Punurai et al., "A shape optimization approach to integrated design and nonlinear analysis of tensioned fabric membrane structures with boundary cables," *International Journal of Solids and Structures*, vol. 83, pp. 114–125, 2016.

[3] B. N. Bridgens and M. J. S. Birchall, "Form and function: the significance of material properties in the design of tensile fabric structures," *Engineering Structures*, vol. 44, pp. 1–12, 2012.

[4] Y. Zhang, Q. Zhang, Z. Yang, L. Chen, and Y. Cao, "Load-dependent mechanical behavior of membrane materials and its effect on the static behaviors of membrane structures," *Journal of Materials in Civil Engineering*, vol. 27, no. 11, Article ID 04015018, 2015.

[5] A. Ambroziak, "Mechanical properties of PVDF-coated fabric under tensile tests," *Journal of Polymer Engineering*, vol. 35, no. 4, pp. 377–390, 2015.

[6] A. Ambroziak, "Mechanical properties of Precontraint 1202S coated fabric under biaxial tensile test with different load ratios," *Construction and Building Materials*, vol. 80, no. 1, pp. 210–224, 2015.

[7] A. Ambroziak and P. Kłosowski, "Mechanical properties for preliminary design of structures made from PVC coated fabric," *Construction and Building Materials*, vol. 50, pp. 74–81, 2014.

[8] A. Ambroziak, "Mechanical properties of polyester coated fabric subjected to biaxial loading," *Journal of Materials in Civil Engineering*, vol. 27, no. 11, Article ID 04015012, 2015.

[9] Y. Zhang, Q. Zhang, and H. Lv, "Mechanical properties of polyvinylchloride-coated fabrics processed with Precontraint® technology," *Journal of Reinforced Plastics & Composites*, vol. 31, no. 23, pp. 1670–1684, 2012.

[10] H. W. Reinhardt, "On the biaxial testing and strength of coated fabrics," *Experimental Mechanics*, vol. 16, no. 2, pp. 71–74, 1976.

[11] S. H. Chen, X. Ding, R. Fangueiro, H. Yi, and X. Yang, "Tensile performance and crack propagation of coated woven fabrics under multiaxial loads," *Journal of Applied Polymer Science*, vol. 113, no. 5, pp. 3388–3396, 2009.

[12] J. W. Chen and W. J. Chen, "Central crack tearing testing of laminated fabric uretek3216LV under uniaxial and biaxial static tensile loads," *Journal of Materials in Civil Engineering*, vol. 28, no. 7, Article ID 04016028, 2016.

[13] Z. Yingying, S. Xiaoguang, Z. Qilin, and L. V. Henglin, "Fracture failure analysis and strength criterion for PTFE-coated woven fabrics," *Journal of Composite Materials*, vol. 49, no. 12, pp. 1409–1421, 2015.

[14] S. H. Chen, X. Ding, and H. L. Yi, "On the anisotropic tensile behaviors of flexible polyvinyl chloride-coated fabrics," *Textile Research Journal*, vol. 77, no. 6, pp. 369–374, 2007.

[15] Z. Zou, J. Han, H. Liu et al., "Orthotropic behavior of PVC architectural membrane materials under tensile loading," *Journal of Zhejiang Sci-Tech University*, vol. 27, no. 2, pp. 186–190, 2010.

[16] J. Cao, R. Akkerman, P. Boisse et al., "Characterization of mechanical behavior of woven fabrics: experimental methods and benchmark results," *Composites Part A: Applied Science and Manufacturing*, vol. 39, no. 6, pp. 1037–1053, 2008.

[17] A. G. Colman, B. N. Bridgens, P. D. Gosling, G.-T. Jou, and X.-Y. Hsu, "Shear behaviour of architectural fabrics subjected to biaxial tensile loads," *Composites Part A: Applied Science and Manufacturing*, vol. 66, pp. 163–174, 2014.

[18] J. Launay, G. Hivet, A. V. Duong, and P. Boisse, "Experimental analysis of the influence of tensions on in plane shear behaviour of woven composite reinforcements," *Composites Science and Technology*, vol. 68, no. 2, pp. 506–515, 2008.

[19] A. Gilat, R. K. Goldberg, and G. D. Roberts, "Experimental study of strain-rate-dependent behavior of carbon/epoxy composite," *Composites Science and Technology*, vol. 62, no. 10-11, pp. 1469–1476, 2002.

[20] A. Martin, R. Othman, and P. Rozycki, "Experimental investigation of quasi-static and intermediate strain rate behaviour of polypropylene glass fibre (PPGF) woven composite," *Plastics, Rubber and Composites*, vol. 44, no. 1, pp. 1–10, 2015.

[21] B. C. Ray, "Effects of changing environment and loading speed on mechanical behavior of FRP composites," *Journal of Reinforced Plastics and Composites*, vol. 25, no. 12, pp. 1227–1240, 2006.

[22] S. Kato, H. Minami, T. Yoshino et al., "Visco-inelastic constitutive equations for fabric membranes based on fabric lattice model-simulations for creep and relaxation compared with experiments," in *Research Report on Membrane Structures*, pp. 29–43, The Membrane Structures Association of Japan, Tokyo, Japan, 1996.

[23] L. Meng and M.-E. Wu, "Study on stress relaxation and creep properties of PTFE membrane," *Journal of Building Materials*, vol. 15, no. 2, pp. 206–210, 2012.

[24] W.-R. Yu, M. S. Kim, and J. S. Lee, "Modeling of anisotropic creep behavior of coated textile membranes," *Fibers and Polymers*, vol. 7, no. 2, pp. 123–128, 2006.

[25] K. J. Kim, W.-R. Yu, and M. S. Kim, "Anisotropic creep modeling of coated textile membrane using finite element analysis," *Composites Science and Technology*, vol. 68, no. 7-8, pp. 1688–1696, 2008.

[26] M. Lei, *Stress Analysis of the Equilibrium Surface for Membrane Structures by Considering Viscoelastic Properties of Coated Fabrics*, Tongji University, Shanghai, China, 2013.

[27] Y. Li and M. Wu, "Uniaxial creep property and viscoelastic–plastic modelling of ethylene tetrafluoroethylene (ETFE) foil," *Mechanics of Time-Dependent Materials*, vol. 19, no. 1, pp. 21–34, 2015.

[28] Y. Zhang, S. Xu, Q. Zhang, and Y. Zhou, "Experimental and theoretical research on the stress-relaxation behaviors of PTFE coated fabrics under different temperatures," *Advances in Materials Science and Engineering*, vol. 2015, Article ID 319473, 12 pages, 2015.

[29] J. Fujiwara, M. Ohsaki, and K. Uetani, "Cutting pattern design of membrane structures considering viscoelasticity of material," in *Proceedings of the IASS Symposium*, pp. 112–113, Nagoy, Japan, October 2001.

[30] H. Nakajima, M. Saitoh, and A. Okada, "Structure analytical study on stress relaxation in tensile membrane structures-structural principle on tensile membrane structure with spring-strut system," in *Research Report on Membrane Structures '07*, pp. 15–25, The Membrane Structures Association of Japan, Tokyo, Japan, 2007.

[31] S. Kato and T. Yoshino, "Simulation for introducing tensions into curved membranes considering both of the cutting pattern method and visco-elasto-plastic characteristics of the fabrics," in *Proceedings of the IASS Symposium*, pp. 110–111, International Association for Shell and Spatial Structures, Nagoya, Japan, 2001.

[32] DIN, "Testing of artificial leather-tensile test," DIN 53354, 1981.

[33] A. K. Sen, *Coated Textiles: Principles and Applications*, CRC Press, 2nd edition, 2007.

[34] Y. Wang, X. G. Chen, R. Young, and I. Kinloch, "Finite element analysis of effect of inter-yarn friction on ballistic impact response of woven fabrics," *Composite Structures*, vol. 135, pp. 8–16, 2016.

[35] H. Wang and Z.-W. Wang, "Quantification of effects of stochastic feature parameters of yarn on elastic properties of plain-weave composite. Part 1: theoretical modeling," *Composites Part A: Applied Science and Manufacturing*, vol. 78, pp. 84–94, 2015.

[36] H. Y. Yeh and L. T. Kilfoy, "A simple comparison of macroscopic failure criteria for advanced fiber reinforced composites," *Journal of Reinforced Plastics and Composites*, vol. 17, no. 5, pp. 406–445, 1998.

[37] S. W. Tsai, "Survey of macroscopic failure criteria for composite materials," *Journal of Reinforced Plastics and Composites*, vol. 3, no. 1, pp. 40–62, 1984.

[38] C. C. Chamis, "Polymer composite mechanics review—1965 to 2006," *Journal of Reinforced Plastics & Composites*, vol. 26, no. 10, pp. 987–1019, 2007.

[39] F. París, "A study of failure criteria of fibrous composite materials," Tech. Rep. NASA/CR-2001-210661, NASA Langley Research Center, Hampton, Va, USA, 2001.

[40] J. Echaabi, F. Trochu, and R. Gauvin, "Review of failure criteria of fibrous composite materials," *Polymer Composites*, vol. 17, no. 6, pp. 786–796, 1996.

[41] H.-Y. Yeh and C. H. Kim, "The Yeh-Stratton criterion for composite materials," *Journal of Composite Materials*, vol. 28, no. 10, pp. 926–939, 1994.

[42] Z. Hashin, "Failure criteria for unidirectional fiber composites," *Journal of Applied Mechanics*, vol. 48, no. 4, pp. 846–852, 1981.